EEET ECOLOGICAL ENGINEERING & ENVIRONMENTAL TECHNOLOGY

Ecological Engineering & Environmental Technology 2024, 25(4), 301–315
https://doi.org/10.12912/27197050/184155
ISSN 2719-7050, License CC-BY 4.0

Received: 2024.02.10
Accepted: 2024.02.22
Published: 2024.02.28

The Removal of Phenol Through Adsorption onto Synthetic Calcium Phosphates – A Study Encompassing Analyses of Kinetics and Thermodynamics

Abdellatif El Bakri[1*], Hicham El Boujaady[1], Nouhaila Ferraa[1], Mounia Bennani-Ziatni[1]

[1] Laboratory of OCCE, Department of Chemistry, Faculty of Sciences, Ibn Tofail University, PB. 133-14050 Kenitra, Morocco

* Corresponding author's e-mail: abdellatif.elbakri@uit.ac.ma

ABSTRACT

The characteristics and suitability of hydroxyapatite (HAP), tricalcium apatite phosphate (PTCa), and octocalcium apatite phosphate (OCPa), which possess similar attributes to those of an ideal adsorbent, were investigated to determine their efficacy in phenol removal. The aim of this paper is to assess the adsorption behavior of phenol on phosphates powders synthesized by the co-precipitation method at ambient temperature. Furthermore, the impact of initial phenol quantities and thermal conditions on the adsorption process was explored. X-ray diffraction analysis revealed the formation of HAP, PTCa, and OCPa structures under room temperature conditions. The sample morphologies were subjected to scrutiny utilizing MEB together with X-ray analysis. Additionally, chemical analysis revealed that Ca/P = 1.6, 1.5, and 1.33 for HAP, PTCa, and OCPa, respectively. The synthesized powders exhibited adsorption abilities of 2.86, 2.74, and 2.52 mg/g for HAP, PTCa, and OCPa, respectively, and reached equilibrium in approximately 80 minutes. The study revealed that the experimental data are appropriately represented by the Langmuir and Freundlich adsorption equations for HAP and PTCa, and Langmuir model in the case of OCPa, as well as by the pseudo-first-order and pseudo-second-order adsorption kinetics. Thermodynamic evaluations, including calculations of $\Delta G°$, $\Delta H°$, and $\Delta S°$, were performed. The results indicated that the adsorption mechanisms exhibited physical characteristics, were thermally absorbing in the case of HAP and exothermic for the other two phosphates, PTCa and OCPa, and occurred spontaneously.

Keywords: HAP; OCPa; PTCa; adsorption equilibrium; reaction rate; thermodynamics; phenol.

INTRODUCTION

Phenol, a widespread organic compound, has been the subject of significant focus in environmental sciences due to its prevalent presence as a pollutant in various ecosystems. This aromatic compound is commonly found in industrial effluents originating from petrochemical, pharmaceutical, and agricultural sectors (Lin et al., 2009; Michałowicz et al., 2007; Rengaraj et al., 2002). Its presence in wastewater and environmental matrices poses considerable ecological concerns due to its toxicity (Dehmani et al., 2020; Mohammadi et al., 2020; Mohammed et al., 2018), persistence, and potential adverse effects on both aquatic life and human health (Wei et al., 2016; Michałowicz et al., 2007). Phenol is known for its detrimental impact on ecosystems, as even trace amounts can disrupt the natural balance of aquatic environments, hindering the growth of aquatic organisms and posing a threat to biodiversity. Its resistance to degradation and tendency to bioaccumulate further accentuate its environmental hazard (Cheng et al., 2016; Li et al., 2019).

Understanding the sources, behavior, fate, and efficient removal of phenol has become imperative in addressing environmental contamination issues. Various scientific endeavours have focused on developing methodologies to mitigate and eliminate phenol from contaminated sites and wastewater

streams, emphasizing the need for effective treatment strategies and innovative technologies.

This introduction aims to delve deeper into the multifaceted aspects of phenol pollution, exploring its sources, environmental impact, and the ongoing efforts in research and technological advancements geared towards mitigating its detrimental effects on ecosystems and human health. Therefore, the effective removal of phenol is essential in preventing water pollution and protecting ecosystems. Adsorption is widely employed as a predominant approach for the purification of water by removing phenol. Various types of adsorbent materials can be employed, such as activated carbon(Hua et al., 2012; Q.S. Liu et al., 2010; Zeboudj et al., 2014), zeolites(Cheng et al., 2016; Tiewcharoen et al., 2021), ion exchange resins, and polymers. These materials possess a high specific surface area (SSA) and chemical properties that facilitate the adsorption of phenol. The process of phenol adsorption involves physicochemical interactions between phenol molecules and the surface of the adsorbent material. These interactions can be electrostatic, hydrophobic, or chemical in nature, depending on the features of both the adsorbent material and phenol itself.

Moreover, the adsorption of phenol offers numerous advantages, including high efficiency, wide availability of adsorbent materials, and ease of implementation. However, it is crucial to acknowledge that adsorption is not a method for phenol destruction but rather a separation technique. Therefore, appropriate management of adsorbent waste is necessary to prevent further contamination. Ongoing research in this field aims to enhance the adsorption efficiency and develop new adsorbent materials that are more efficient and environmentally friendly. In this study, the focus is on phosphocalcic apatite-based supports, namely hydroxyapatite (HAP), tricalcium apatite phosphate (PTCa), and octocalcium apatite phosphate (OCPa), which serve as the adsorbents of interest.

The aim of this study is to conduct an in-depth investigation into the adsorption capacity of phenol from aqueous solutions using three synthetic phosphocalcic apatite materials, namely HAp, PTCa, and OCPa. Various experimental factors, including initial adsorbate concentration, contact time, and temperature (T), were examined to understand their influence on the adsorption process. The results were evaluated using kinetic and isotherm models, while thermodynamic parameters such ΔH, ΔS, and ΔG were analyzed.

MATERIALS AND METHODS

Adsorbent

Adsorption experiments were performed on three calcium phosphates, namely HAP, PTCa, and OCPa:

- HAP – the preparation of stoichiometric hydroxyapatite ($Ca_{10}(PO_4)_6(OH)_2$) involves a slow precipitation process in a basic medium. It is a double decomposition reaction between a solution of calcium nitrate and a solution of ammonium phosphate. The solution A of phosphate is prepared by dissolving 26 g of ($(NH_4)_2HPO_4$) in 1300 ml of decarbonated distilled water. The calcium nitrate solution (solution B) is obtained by dissolving 47g of ($Ca(NO_3)_2$,$4H_2O$) in 0.55 L of decarbonated pure water. A concentrated ammoniacal solution is prepared, without dilution, to regulate the pH of the medium. Solution A and 1500 ml of the ammonia solution are simultaneously pumped into the boiling solution B using a peristaltic pump, while maintaining a constant stirring speed of 150 rpm. The presence of excess ammonia is essential to establish an alkaline environment with a pH of 9. Following the completion of the addition, the mixture is subjected to boiling and stirring for approximately 30 minutes. The deposit obtained is subjected to hot-filtration using a Buchner funnel, followed by rinsing with a solution comprising one liter of deionized water and 30 mL of ammonia. Subsequently, the precipitate is dried overnight at 80 °C (El Bakri et al., 2024; El Rhilassi et al., 2012; Mourabet et al., 2015).
- PTCa – the tricalcium apatitic phosphate ($Ca_9(HPO_4)(PO_4)_5(OH)$) is a solid with a Ca/P atomic ratio of 1.5 and a high SSA. It was obtained using the method developed by Heughebaert. This involves a co-precipitation process using a solution A of calcium nitrate and a solution B of ammonium phosphate, following the following protocol: Solution A: 23.5 g of ($Ca(NO_3)_2$,$4H_2O$) is dissolved in 225 ml of distilled water containing 40 ml of ammonia (density = 0.92). The pH value of this solution is approximately 11.2. Solution B: 13 g of $(NH_4)_2HPO_4$ is dissolved in 650 ml of H_2O. To the solution, 20 mL of ammonia (density = 0.92) is introduced, resulting in an approximate pH of 9.9 for this solution. Solution A is

rapidly poured into solution B at room temperature, and a white precipitate appears. The precipitate is isolated from the mother solution through filtration, followed by immediate washing with a alkaline solution comprising 1.5 liters of water and 7.5 mL of ammonia. Subsequently, the precipitate is dried in an oven at 80 °C for a duration of 24 hours (El Boujaady et al., 2011, 2014, 2017).

- OCPa – octocalcium apatitic phosphate ($Ca_8(HPO_4)_{2.5}(PO_4)_{3.5}(OH)_{0.5}$) was synthesized using the method described by Zahidi. This method involves the precipitation of the phosphate through a rapid double decomposition reaction between a calcium salt solution (solution A) and an ammoniacal solution of orthophosphate ions in a water/ethanol medium (solution B). The presence of ethanol, which induces a decrease in the dielectric constant, promotes protonated species such as HPO_4^{2-} ions and stabilizes amorphous calcium phosphates. A calcium salt solution (A) is prepared by dissolving 7.09 g of Ca(NO3)2·4H2O in 100 mL of distilled water, followed by the addition of 100 mL of ethanol (density = 0.79). Phosphate solution (B): 3.96 g of diammonium hydrogen phosphate $(NH_4)_2HPO_4$ is dissolved in 250 ml of distilled water. To this solution, 45 ml of an ammonia solution (density = 0.92) and 295 ml of ethanol (density = 0.79) are sequentially added. The co-precipitation process is conducted at a T of 37 °C by swiftly pouring solution A into solution B while maintaining stirring. Following formation, the resulting precipitate is separated from the mother solution through filtration using a Buchner funnel. Subsequently, the precipitate is washed with a basic solution comprising 180 mL of degassed deionized water, 30 mL of an ammonia solution (density = 0.92), and 210 mL of ethanol (density = 0.79), with the volume percentage of ethanol approximately 50%. Lastly, the precipitate is dried overnight in an oven at 80°C (El Boujaady et al., 2011).

The SSA was determined through the application of the BET method, where N_2 adsorption at 77 K was employed. The scanning electron microscopy (MEB) images were obtained through the use of a Quantros Fei Thermo Fisher Scientific scanning electron microscope coupled with energy-dispersive X-ray analysis. The X-ray powder diffraction (XRD) pattern was acquired employing a Panalytical X Pert 3 Powder diffractometer equipped with copper Ka radiation (Kα1 = 1.5405980 Å).

Adsorption experiments

Adsorbate

To create a stock solution of phenol, pure samples of the solute were dissolved in distilled water. Batch adsorption studies for a single solute system were conducted in a test tube. In these studies, 10 ml of a known concentration solution of phenol was used to investigate equilibrium isotherms and the impact of varied factors including kinetics, pH, initial concentration, and adsorbent dose on the adsorption of phenol onto phosphates. The concentration of phenol was determined using a UV spectrophotometer (UV-2005, Selecta, Spain) employing the method involving 4-aminoantipyrine (Fiamegos et al., 2002; Norwitz et al., 1981) was employed to evaluate the quantity of phenol adsorbed. This method forms colored complexes with certain phenolic compounds. The batch process involved combining 5 ml of the NH_4Cl-NH_4OH buffer solution with 50 ml of the phenol solution to be analyzed. The solution's pH was adjusted to 9.5 using the NH4Cl-NH4OH buffer solution. Subsequently, 1.0 ml of the 4-aminoantipyrine solution was added to 2.0 ml of $K_3[Fe(CN)_6]$ solution. The resulting mixture was carefully subjected to agitation and subsequently allowed to reach equilibrium at ambient T for 5 minutes (Tang et al., 2015; T. Wang et al., 2017). The absorbance of the resulting solution was then assessed by employing the spectrophotometer at 511 nm.

Experimental protocol

The study of phenol adsorption by synthetic phosphates (HAP, PTCa and OCPa) was conducted in a static mode (batch). For each experiment, the solid was brought into contact with a phenol solution. The blend was agitated consistently at a fixed rate of 500 rpm for a duration of one minute before being transferred to a T-regulated water bath set at 25 °C. The solid is subsequently isolated from the colloid via separation utilizing a fritted glass apparatus. The concentration of phenol is assessed employing a UV-visible spectrophotometer. The amount of phenol adsorbed by the adsorbent is

quantified by the subsequent equation (X. Liu et al., 2021; Mishra et al., 2021; Nakhjiri et al., 2021a) :

$$Qt = \frac{(C0-Ct)V}{m} \quad (1)$$

where: Qt – amount of phenol in mg/g of adsorbent, C_0 – represents the initial concentration, while Ct signifies the concentration of phenol at time t (mg/l), V – volume of the solution (l), m – quantity of adsorbent employed (g).

The simplicity in their application makes the classical Langmuir (Langmuir., 1916) (Eq. 2) and Freundlich (Freundlich, 1926) (Eq. 3 and 4) models, which describe monolayer formation, valuable. So, by utilizing the linearized Langmuir equation (Langmuir., 1916), we were able to ascertain the key adsorption parameters: the saturation adsorption capacity represented by Q∞, and the constant interaction between the adsorbate and adsorbent denoted as b.

$$1/Qad = 1/(bQ\infty)Ceq + 1/Q\infty \quad (2)$$

$$Y = aXm \text{ with } m \leq 1 \quad (3)$$

Let Y represent the amount of the substance adsorbed per unit surface area or mass of the adsorbent, and X represent the equilibrium concentration of the adsorbate in the solution. The parameters a and m establish the relationship between the adsorbent and adsorbate. By linearly transforming the equation, we derive the following expression:

$$log(Y) = log(a) + mlog(X) \quad (4)$$

The relationship between the logarithm of Y and the logarithm of X helps to determine m and a. It's important to note that at very low levels of adsorption, the Freundlich's law typically describes the adsorption mode. Conversely, when there's a high recovery rate, the Langmuir's law accurately describes this process.

pH study

In a 10 ml test tube containing a phenol solution, phosphate (HAP or PTCa or OCPa) was introduced. The initial concentration of phenol was uniformly set to 100 mg/L for all experimental conditions. In order to manipulate the pH, HCl (0.1 M) and NaOH (0.1 M) were employed. After mixing the components, the mixture was stirred for two minutes and then transferred to a thermostatic bath maintained at a constant T of 25 °C. Following a contact period of 5 hours, the solid particles were separated from the liquid solution by filtration using a porous glass material. Additionally, the pH of the solution was measured.

RESULTS AND DISCUSSION

Adsorbent

The HAP, PTCa and OCPa phosphate samples respectively have a SSA of approximately 137; 62 and 58 m^2/g. The X-ray diffraction patterns of the prepared samples (Figure 1) indicate that the obtained phases have an apatitic structure with poor crystallinity. The apparent dimensions of the crystallites, determined using the Scherrer equation (1918), for the two examined peaks (002) and (310) in Figure 1 are 415 and 175 Å, respectively (Figure 1a), 415 and 107 Å (Figure 1b), and 415 and 128 Å (Figure 1c). These values demonstrate that the crystals of HAP, PTCa, and OCPa are elongated along the c-axis, with L(002) > L(310).

Figures 2a, 2c, 3a, 3c, 4a, 4c present the MEB images, before and after adsorption of phenol by HAP, tricalcium phosphate apatitic and apatitic octocalcium respectively. The changes in the surface morphology of HAP, PTCa and OCPa before and after adsorption may indicate the adsorption of phenol on the adsorbents. The presence of a line attributed to carbon on the EDX spectrum of HAP, PTCa and OCPa after the adsorption of phenol (Figure 2d, 3d and 4d) can confirm the adsorption of phenol on HAP, tricalcium apatitic phosphate and octocalcium apatitic phosphate.

The pH (pH (final) – pH (initial)) as a function of the adjusted initial pH (Figure 5) gives pHpzc of 6.25, 5.85 and 5.45 respectively for HAP, PTCa and OCPa, indicating that for higher pH values the surface is negatively charged, whereas for pH values below than pHpzc the surface exhibits a positive charge.

Influence of pH on the adsorption equilibrium of phenol onto HAp, PTCa, and OCPa

Figure 6 depicts the impact of pH on the adsorption of phenol by HAp, PTCa, and OCPa. The results clearly demonstrate a significant effect of pH on the adsorption process. The adsorption capacity of phenol shows a decreasing trend as the pH increases, reaching its lowest point at a pH value of 6.12 for HAp and PTCa, and 5 for OCPa. Beyond these pH values, the adsorption capacity slightly increases. The maximum adsorption is

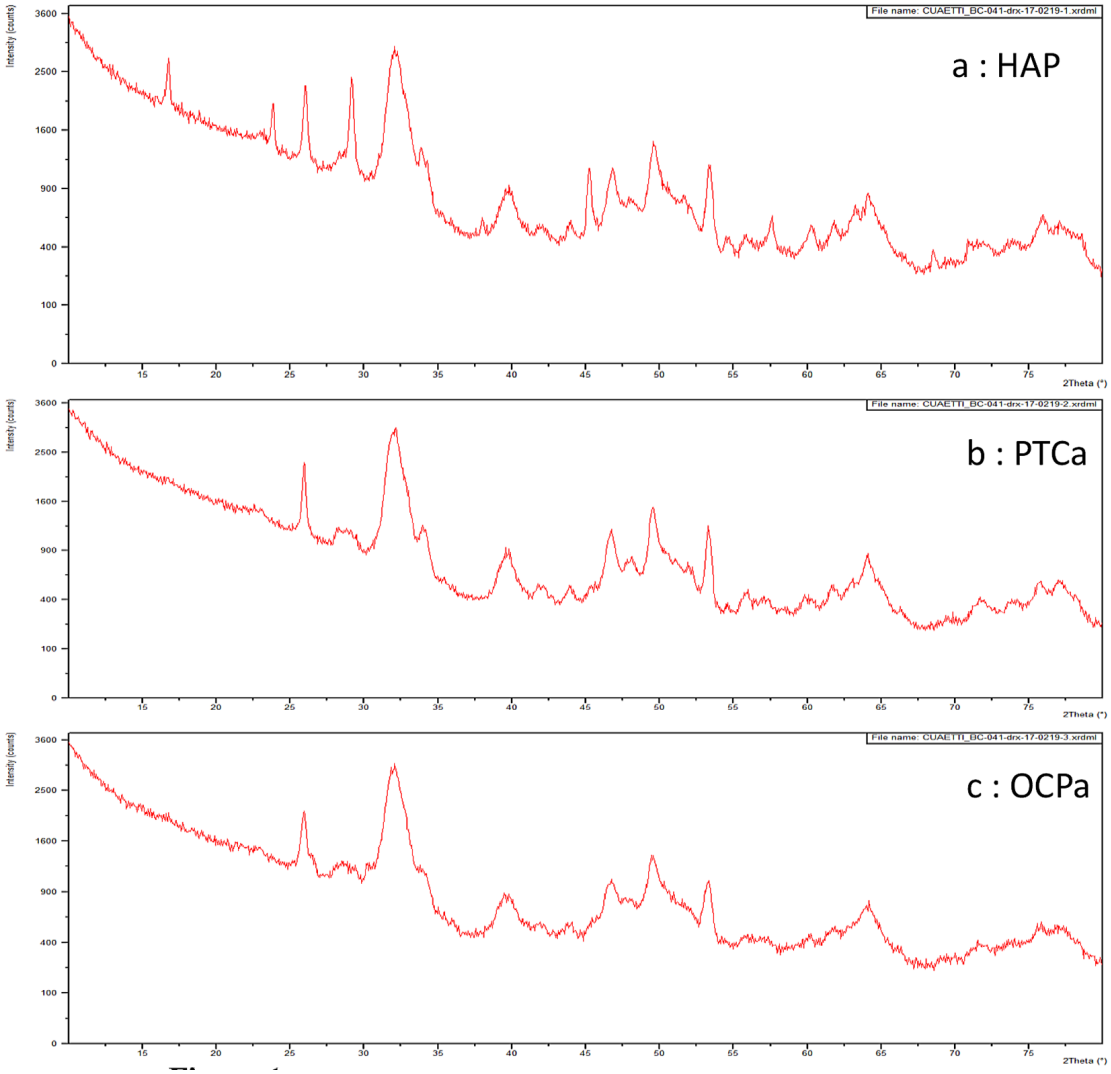

Figure 1. XRD patterns of synthesized HAP, PTCa and OCPa

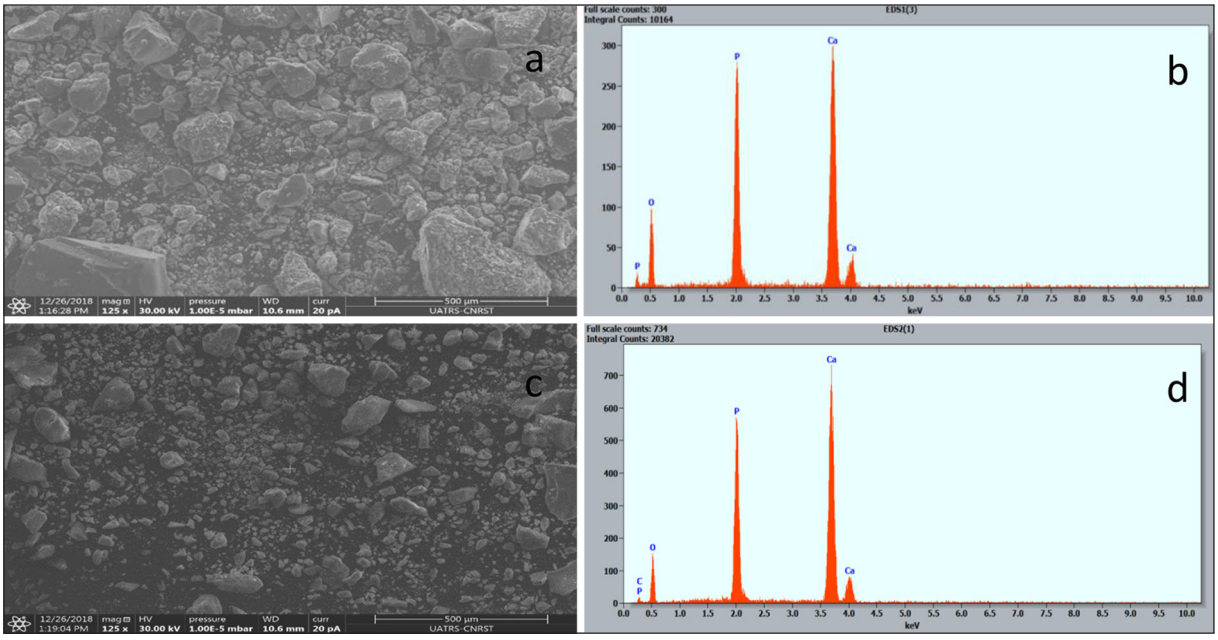

Figure 2. MEB images of (a) HAp and (c) HAP/phenol and EDAX spectra of (b) HAP and (d) HAp/phenol

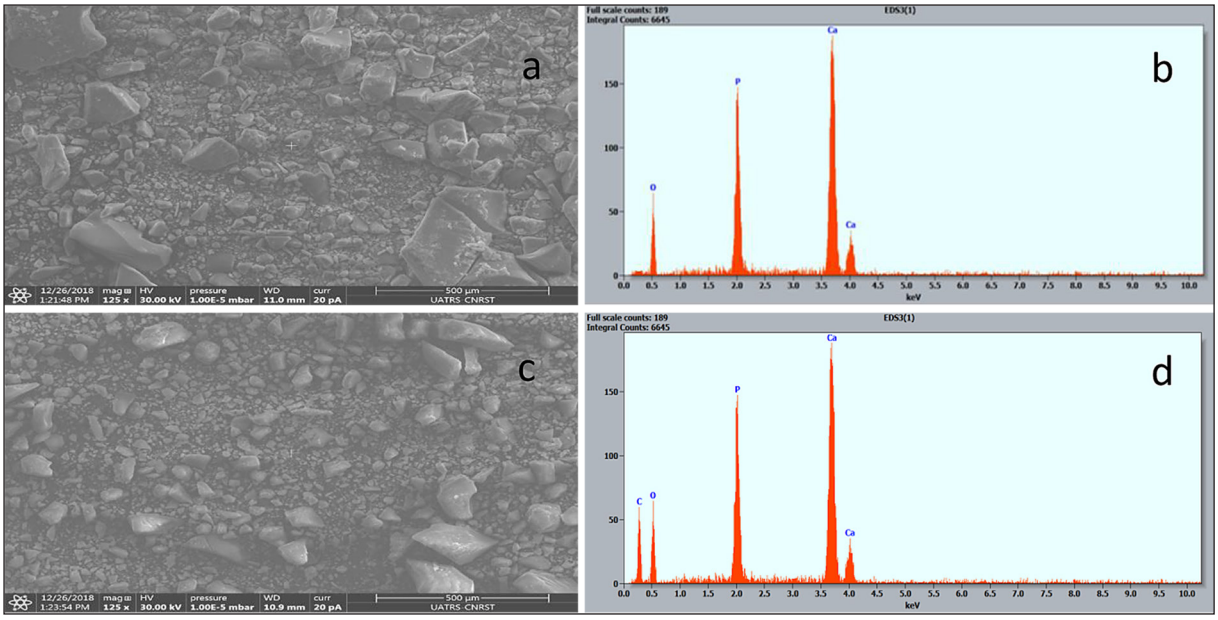

Figure 3. MEB images of (a) PTCa and (c) PTCa/phenol and EDAX spectra of (b) PTCa and (d) PTCa/phenol

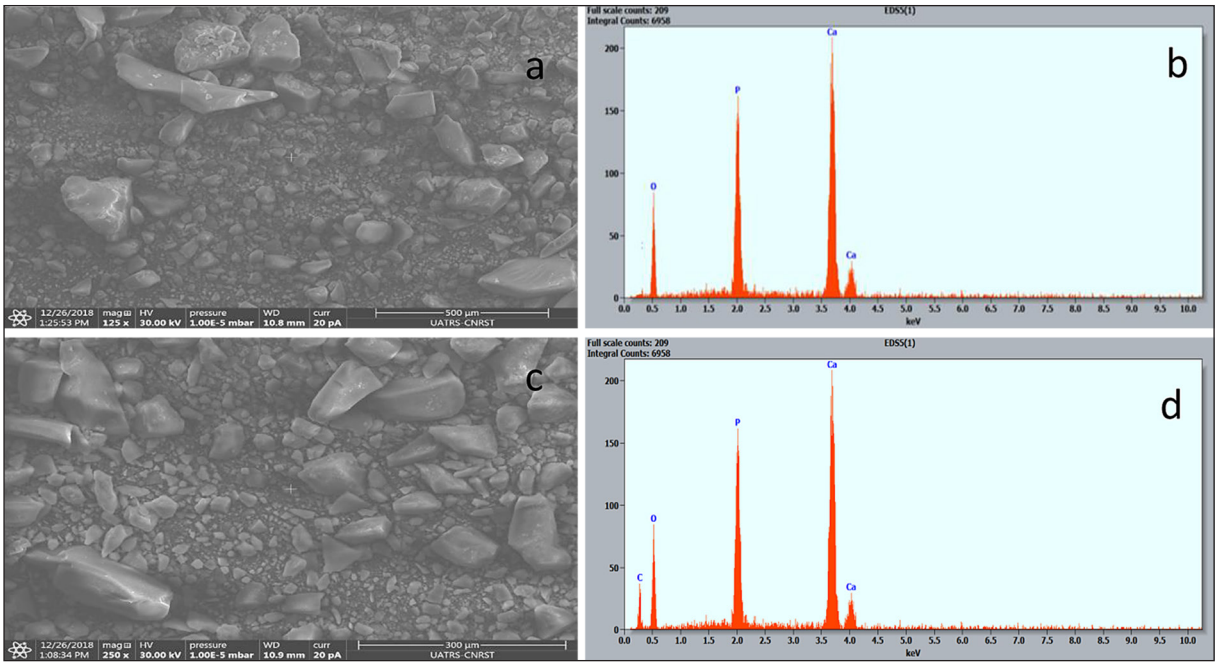

Figure 4. MEB images of (a) OCPa and (c) OCPa/phenol and EDAX spectra of (b) OCPa and (d) OCPa/phenol

recorded at pH 3.5 with values of 3.47, 3.23, and 2.31 mg/g for the three adsorbents HAp, PTCa, and OCPa, respectively.

This observation can be rationalized by considering the zero charge points (pHz) of the three adsorbents, HAP, PTCa, and OCPa, established at 6.25, 5.85, and 5.45, respectively. Once the pH of the solution exceeds the pHz threshold, the surface of the adsorbent particles (HAp, PTCa, and OCPa) acquires a negative charge. Conversely, when the pH is below the pHz, the surface becomes positively charged.

As a result, the absorbate-adsorbent interactions of phenol with negatively charged HAp, PTCa, and OCPa particles gradually become significant for pH values lower than pHz. Conversely, in environments with pH values higher than pHz and under strongly basic conditions, where phenol exists in its deprotonated and ionized form, the ionic strength is altered accordingly,

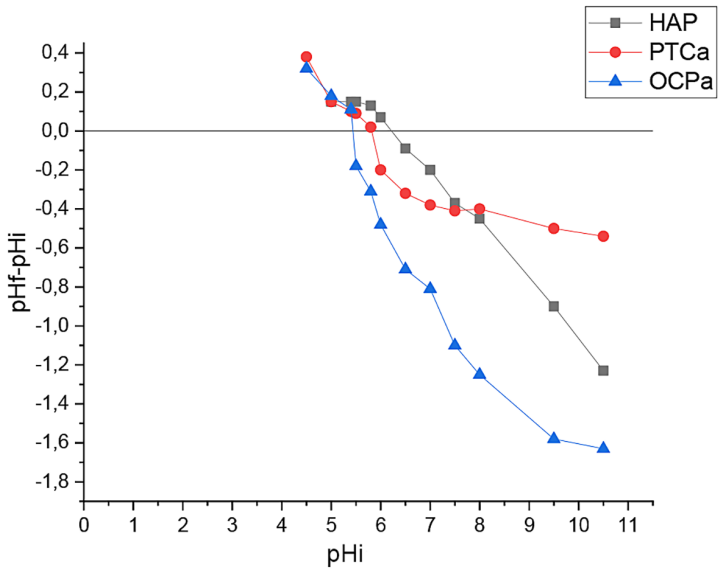

Figure 5. Identification of the zero point of charge of HAp, PTCa and OCPa

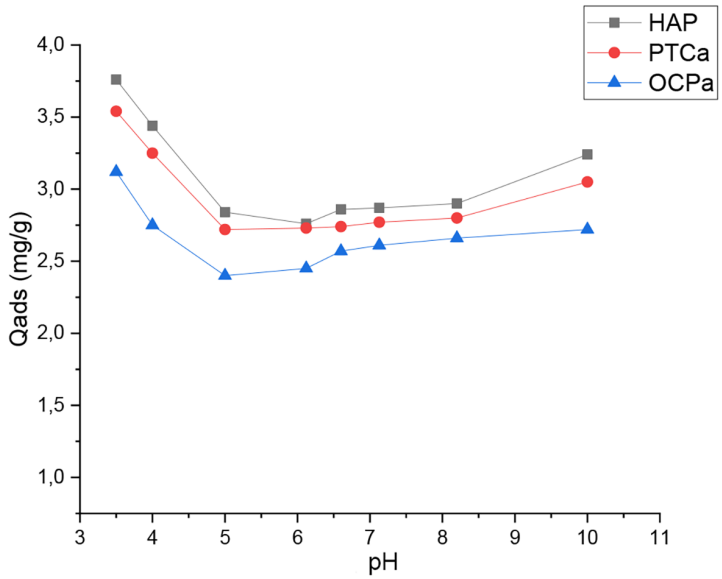

Figure 6. Effect of pH on the equilibrium adsorption phenol onto HAp, PTCa and OCPa

leading to relatively enhanced adsorption. Lin et al. (Lin et al., 2009) observed a similar trend in phenol adsorption behavior in HAP, which corroborates our findings.

Adsorption kinetics (AK)

Equilibrium was rapidly established, with phenol reaching its maximum adsorption within 80 minutes of contact (Figure 7) for all three adsorbents. This fixation can be ascribed to the initial abundance of active sites, despite a subsequent decline in the proportion of adsorption sites over time. In Figure 7, the AK of phenol on HAp, PTCa, and OCPa are depicted at a specific organic concentration of 100 mg/L. Based on this information, the approximate time to reach equilibrium for the phenol-apatite adsorption system can be determined to be around 80 minutes for all three phosphates, HAp, PTCa, and OCPa, under the specified test conditions.

AKs were assessed using Lagergren (Lagergren et al., 1898) (eq. 5), (eq. 6), (eq. 7), and the intraparticle diffusion model (eq. 8).

$$log(Qe - Qt) = log(Qe) - K1/2.3t \quad (5)$$

The model proposed by Ho and McKay in 1999 and 2000 (Ho & Mckay, 2000, 1999), known

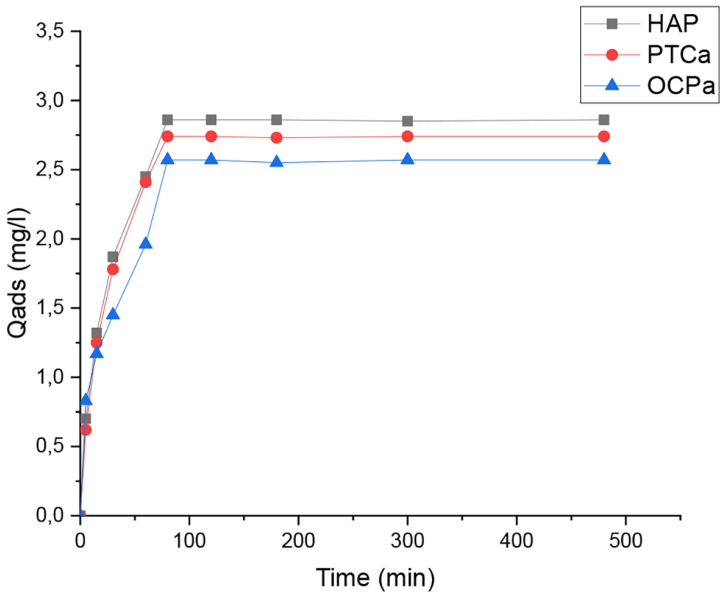

Figure 7. AK of phenol onto HAp, PTCa and OCPa (200 mg of solid, an initial phenol concentration of 100 ml/l, starting pH, at 298 K, stirred for 1 minute)

as the pseudo second order model, has been investigated to understand the adsorption mechanism.

$$t/Q_t = 1/2K_2Q_e2 + t/Q_e \quad (6)$$

$$1/(Q_e - Q_t) = 1/Q_e + K_3t \quad (7)$$

In the given equation, Qe represents the quantity of adsorbate at equilibrium (in mg/g), while t represents the contact time. The rate constants K1, K2, and K3 correspond to the adsorption rates. To determine the rate of intraparticle diffusion, as proposed by Weber and Morris in 1963, the initial intra-particle transport rate can be calculated by plotting Q_t against $t^{½}$:

$$q_t = k_p t^{1/2} + C \quad (8)$$

where: q_t represents the amount of solute adsorbed on the surface of the sorbent at time t (mg/g), k_p represents the intra-particle rate coefficient (mg g^{-1} $min^{0.5}$), t signifies the time (in minutes), and C (mg/g) is a constant indicating the thickness of the boundary layer.

The intraparticle diffusion model was utilized to determine the dominant step in the adsorption process. According to the Weber and Morris theory, a linear regression of Q_t against $t^{1/2}$ that passes through the origin would indicate that intraparticle diffusion exclusively controls the process. However, as shown in Figure 8b, the regression was not linear, and the plot did not originate from the origin for all three adsorbents (HAP, PTCa, and OCPa). This indicates that intraparticle diffusion alone did not govern the adsorption process for the studied phosphates.

The adsorption rate constants of phenol on HAp, PTCa, and OCPa were determined graphically for the pseudo-first order, pseudo-second order, and second-order models (Figures 8a, 8c, and 8d). The determination of the different rate constants (shown in Table 1) demonstrates that the pseudo-first order and pseudo-second order models exhibit high correlation coefficients (HAp: R2=0.999/0.998; PTCa: R2=0.998/0.998; and OCPa: R2=0.995/0.997) is the most reliable.

Adsorption isotherms studies

The study examined the adsorption characteristics of phenol on phosphate by exposing 200 mg of adsorbent to 10 ml of various solutions with phenol concentrations spanning from 40 to 500 mg/l and a duration of 4 hours.

Figure 9 illustrates the relationship between the quantity of adsorbate and the concentration within the medium. It is clear that the amount of phenol absorbed increases significantly with different concentrations of the solution medium until it reaches a plateau for all three adsorbents, indicating a form of monolayer adsorption. The adsorption isotherms are represented using the Freundlich and Langmuir models in Figure 10. Based on the correlation coefficient values (refer to Table 3), both the Freundlich and Langmuir

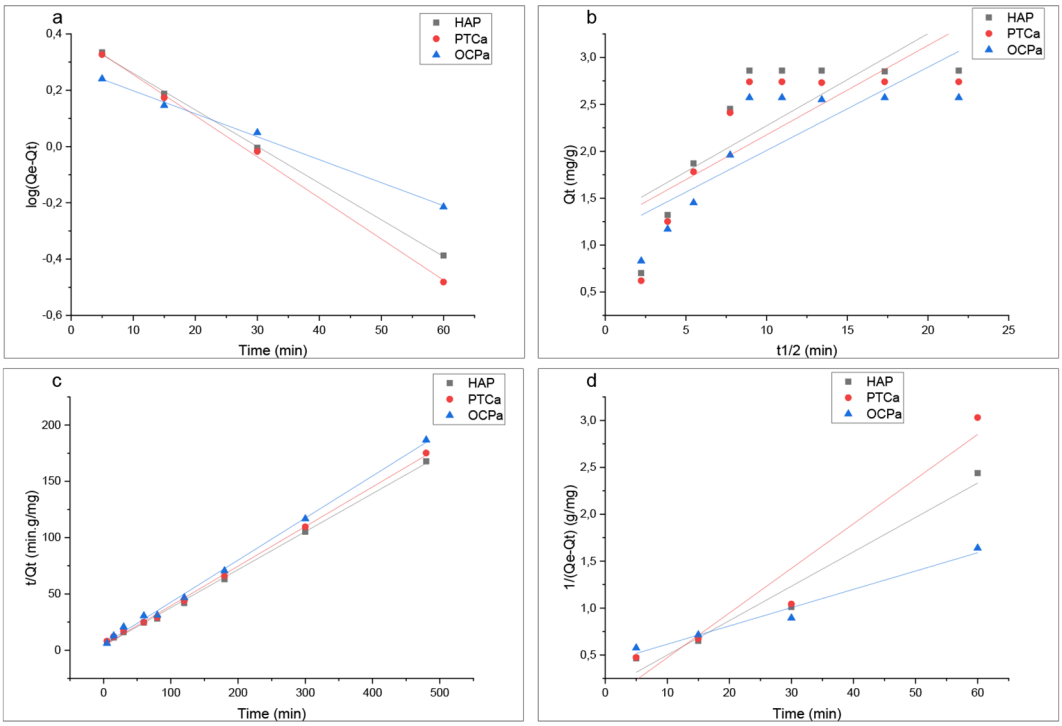

Figure 8. AK of phenol on HAP, PTCa and OCPa conducted at 25°C (initial phenol concentration: 100 mg/l, pH: 6.66, 200 mg of solid, stirring duration: 1 minute)

Table 1. Kinetic parameters associated with the adsorption of phenol onto HAp, PTCa and OCPa

Adsorbents	Pseudo-first order		Pseudo-second order		Second order		Intra-particle diffusion		
	k_1 (min^{-1})	R2	k_2 ($g/mg.min^{-1}$)	R2	k_3 ($min^{-1}.g/mg$)	R2	kp ($g.mg^{-1}.min^{0.5}$)	C ($mg.g^{-1}$)	$R2$
HAP	0.0299	0.999	0.0143	0.998	0.0367	0.947	0.0982	1.29	0.549
PTCa	0.0336	0.998	0.0146	0.998	0.0476	0.914	0.0954	1.22	0.538
OCPa	0.0188	0.995	0.0134	0.997	0.0195	0.959	0.0888	1.12	0.613

Table 2. Quantification of adsorbed phenol amount

Quantification		Adsorbent		
		HAP	PTCa	OCPa
Qe exp (mg/g)		2.86	2.74	2.52
Qe cal (mg/g)	Pseudo-first order	2.46	2.52	1.91
	Pseudo-second order	2.96	2.84	2.67
	Second order	7.58	-203.25	2.39

models adequately describe the adsorption isotherms on HAP and PTCa. However, the apatitic octocalcium phosphate best fits the Langmuir model. The determined Q_1 adsorption capacities, which represent the maximum adsorption capacities with full monolayer coverage, are 13.90 mg/g for HAP, 14.55 mg/g for PTCa, and 4.73 mg/g for OCPa, respectively.

Thermodynamics

In Figure 11, the variation of the adsorbed quantity with respect to T is depicted. The results show that as T increases, the equilibrium adsorption capacity of phenol increases for HAP, but decreases for PTCa and OCPa. This indicates that within the T range of 293 to 323 K, the rise in the

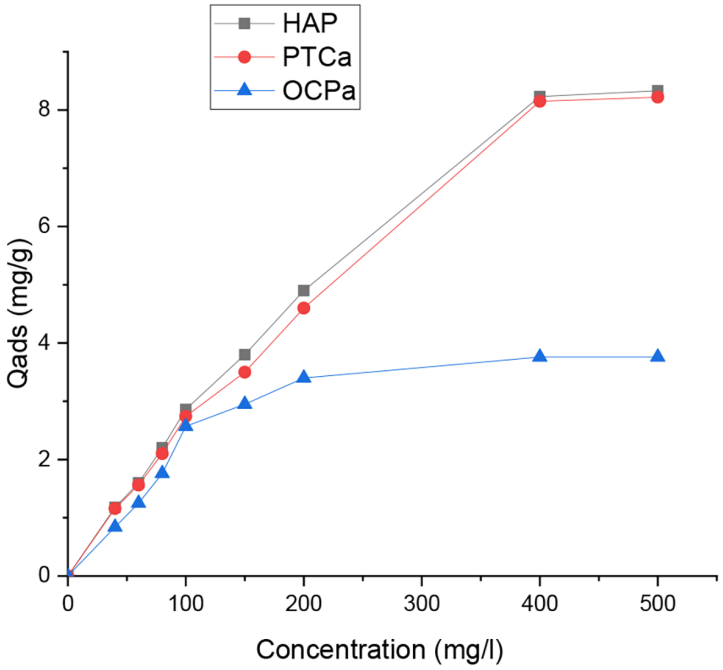

Figure 9. Isotherms depicting the adsorption of phenol on HAP, PTCa and OCPa (solid mass: 200 mg, agitation time: 1 minute, T: 298 K)

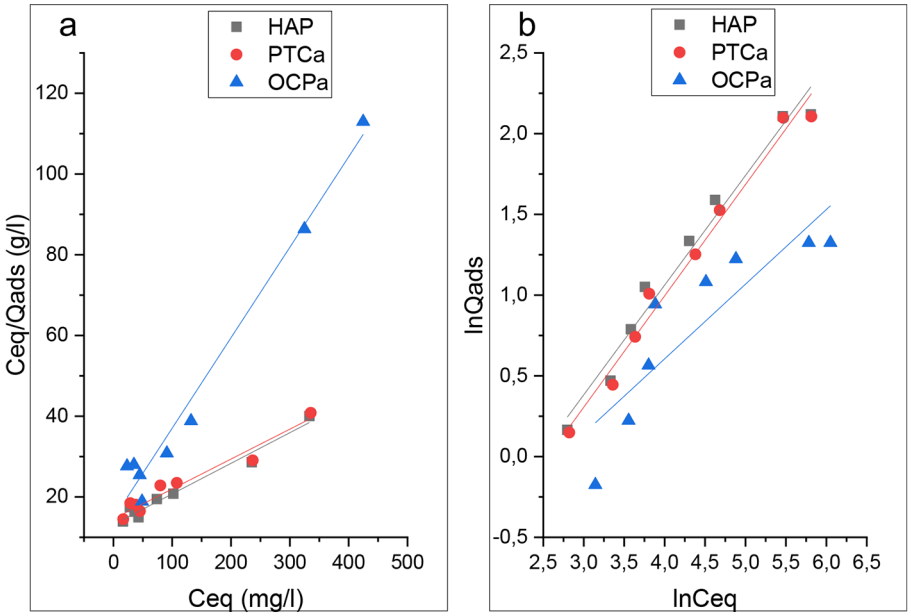

Figure 10. Modeling the adsorption isotherm of phenol onto phosphate (HAP, PTCa and OCPa) using (a) the Langmuir model and (b) the Freundlich model

adsorbed quantity for HAP can be attributed to the endothermic nature of the adsorption process. On the other hand, for PTCa and OCPa, the adsorbed quantity decreases as the T increases within the same T range, indicating that adsorption is an exothermic process for these two adsorbents. According to literature, the thermodynamic factors associated with the adsorption process, such as ΔH, ΔG) and ΔS, can be computed by utilizing the subsequent equations (Alves et al., 2020; Konggidinata et al., 2017; Zulfiqar et al., 2020):

$$\Delta G = -RTLnKc \quad (9)$$

$$\Delta G = \Delta H - T\Delta S \quad (10)$$

$$LnKc = \Delta S/R - \Delta H/RT \quad (11)$$

Table 3. Parameter values for the fitting of Freundlich and Langmuir models

Adsorbents	Freundlich			Langmuir		
	m	*a* (l/g)	R^2	Q_∞ (mg/g)	*b* (l/g)	R^2
HAP	0.6792	0.02212	0.97	13.90	0.0051	0.97
PTCa	0.6896	0.01725	0.98	14.55	0.0043	0.94
OCPa	0.4625	0.05688	0.73	4.73	0.0107	0.98

$$Kc = \frac{(C0 - Ceq)}{Ceq} \tag{12}$$

where: Kc – represents the equilibrium constant, ΔG – stands for Gibbs free energy (J/mole), ΔH – denotes enthalpy (J/mole), ΔS – signifies entropy (J/mol K), T – represents the absolute $T(K)$, R(8.314 J/mol K) signifies the gas constant and C_0 indicates the initial concentration of the adsorbate while C_{eq} denotes the concentration at equilibrium.

A linear relationship between *ln Kc* and 1/T was observed for an initial phenol concentration of 100 mg/l, as depicted in Figure 12. Using the slope and intercept obtained from this plot, the values for ΔH and ΔS were derived and are elaborated upon in Table 4.

The positive ΔS value in the case of HAP indicates an increase in randomness during the process (Hameed et al., 2007; Mahmoodi et al., 2011) on the other hand the negative value of ΔS accompanying the adsorption of phenol on the two phosphates other phosphates PTCa and OCPa show that we have achieved a more orderly system. Furthermore, the ΔH values for all phosphates studied are less than 40 Kj/mol suggesting that the adsorption of phenol on these phosphates mainly involves physisorption processes.

The ΔG values for all three phosphates (as shown in Table 4) fall within the range of 0 to -20 kJ/mol. This suggests that physisorption is the dominant mechanism, as the free energy variation for chemisorption is generally much larger, ranging from -80 to -400 kJ/mol.

Additionally, Von Oepen (Yon Oepen et al., 1991) determined the free energy of adsorption for various types of interactions. The free energy for Van der Waals forces typically ranges from 4 to 10 kJ/mol, while hydrogen bonding falls within the range of 2 to 40 kJ/mol. Chemical bonding, on the other hand, exceeds 60 kJ/mol. Based on the values obtained (presented in Table 4), it is likely that the adsorption mechanisms of phenol onto the different phosphates can be attributed to hydrogen bonding.

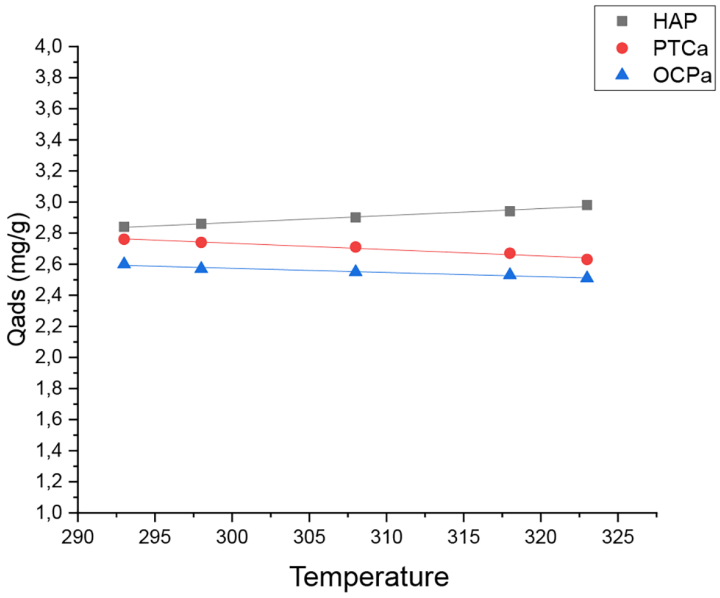

Figure 11. Impact of T on the adsorption of phenol onto HAp, PTCa and OCPa (with a solid quantity of 200 mg, initial phenol content of 100 mg/l, initial pH, stirring time of 1 minute, and contact time of 4 hours)

Table 4. Thermodynamic parameters of phenol adsorption onto phosphate powders (HAP, PTCa, and OCPa)

Support	*T*(*K*)	*Kc*	Δ*G* (KJ/mol)	Δ*H* (KJ/mol)	Δ*S* (J/mol K)	*R*2
HAP	293	1.31	-0.67	2.879	12.072	0.974
	298	1.34	-0.72			
	308	1.38	-0.83			
	318	1.43	-0.94			
	323	1.48	-1.04			
PTCa	293	1.23	-0.51	-2.575	-7.024	0.959
	298	1.21	-0.48			
	308	1.18	-0.43			
	318	1.15	-0.36			
	323	1.11	-0.28			
OCPa	293	1.08	-0.19	-1.698	-5.176	0.958
	298	1.06	-0.14			
	308	1.04	-0.10			
	318	1.02	-0.06			
	323	1.01	-0.02			

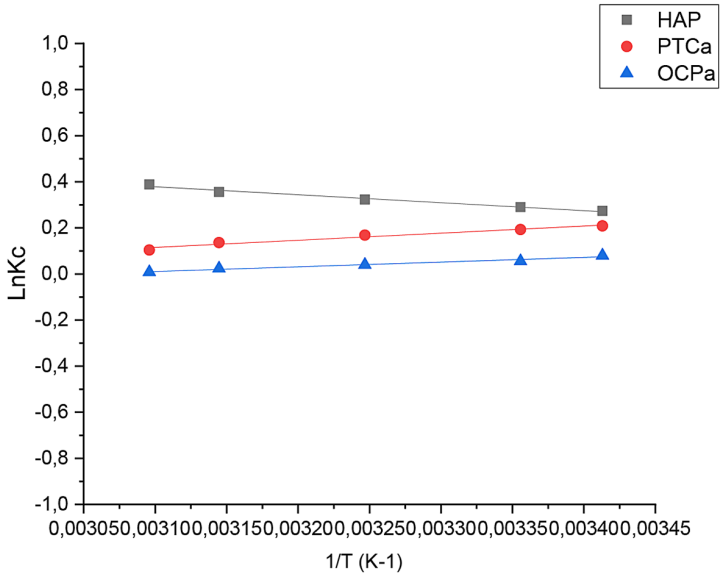

Figure 12. Van't Hoff graphical approach

Comparative analysis with previously reported adsorbents

Over the past decade, substantial progress has been achieved in the field of adsorbents and their adsorption capabilities, resulting in the development of innovative technologies and materials offering improved performance in the removal of phenol contaminant. The aim of the comparative study on six Hap adsorbents, Q_{ads}= 8.33 mg·g^{-1} (this study) PTCa Q_{ads}= 8.22 mg·g^{-1} (this study); OCPa, Q_{ads}= 3.76 mg·g^{-1} (this study); AC-AL_2O_3 (Q_{ads} = 3.546 mg·g^{-1}) (Abussaud et al., 2016); GO/GER (Q_{ads}= 25.45 mg·g^{-1}) (X. Wang et al., 2018); AC from eggshell (Q_{ads} = 192 mg·g^{-1}) (Giraldo & Moreno-Piraján, 2014); Peanut shells (Q_{ads} = 16.84 mg·g^{-1}) (Villar da Gama et al., 2018); Scoria Stone (Q_{ads} = 67.11 mg·g^{-1}) (Sharafi et al., 2019) and DNNH (Q_{ads} = 21.19 mg·g^{-1}) (Nakhjiri et al., 2021b) consists of evaluating the progress made and identifying the most effective adsorbents. The results obtained highlight notable differences between these adsorbents. First, AC from eggshell adsorbent demonstrated exceptional adsorption capacity, effectively capturing contaminants. This

remarkable efficiency may be linked to its large SSA and its strong affinity for the targeted substances. Conversely, the DNNH adsorbent had a slightly lower adsorption capacity but remained effective for phenol removal. The scoria stone adsorbent, however, exhibited moderate adsorption capacity and comparatively lower efficiency. The adsorbents AC-AL_2O_3, OCPa, PTCa, and HAP exhibited relatively low adsorption capacities, placing them at the lower end of our comparative ranking. These results highlight the importance of selecting an appropriate adsorbent based on the specific application requirements, taking into account the adsorption capacity necessary for successful contaminant removal.

CONCLUSIONS

In conclusion, the adsorption of phenol onto phosphate powders shows great promise as a water decontamination method for phenolic compounds. Phosphates, especially HAP, exhibit high phenol adsorption capacities due to their crystalline structure, large SSA, and favorable chemical properties. The interaction between functional groups in phosphates and phenol molecules enables efficient retention of phenol within the phosphate powders. However, certain considerations should be taken into account. Proper preparation of phosphate powders, including particle size and purity, is crucial for optimizing phenol adsorption. Additionally, experimental conditions such as initial phenol concentration, pH, and contact time need careful control to maximize adsorption efficiency.

The adsorption process onto HAP and PTCa is well described by the Freundlich and Langmuir models, and the Langmuir model is suitable for OCPa, indicating favorable adsorption behavior. Kinetic studies show relatively rapid attainment of equilibrium, following a pseudo-first-order and pseudo-second-order mechanism for all three phosphates studied. Moreover, increasing the T enhances the maximum adsorption capacity for HAP, indicating a correlation between thermodynamic factors and the adsorption process. Thermodynamic analysis suggests that phenol adsorption onto HAP involves both physisorption and endothermic processes, while for tricalcium apatite phosphate and octocalcium apatite phosphate, the adsorption is physisorption-based and exothermic.

REFERENCES

1. Abussaud, B., Asmaly, H.A., Ihsanullah, Saleh, T.A., Gupta, V.K., Laoui, T., Atieh, M.A. 2016. Sorption of phenol from waters on activated carbon impregnated with iron oxide, aluminum oxide and titanium oxide. Journal of Molecular Liquids, 213, 351–359. https://doi.org/10.1016/j.molliq.2015.08.044
2. Alves, D.C.S., Coseglio, B.B., Pinto, L.A.A., Cadaval, T.R.S. 2020. Development of Spirulina/chitosan foam adsorbent for phenol adsorption. Journal of Molecular Liquids, 309. https://doi.org/10.1016/j.molliq.2020.113256
3. Cheng, W.P., Gao, W., Cui, X., Ma, J.H., Li, R.F. 2016. Phenol adsorption equilibrium and kinetics on zeolite X/activated carbon composite. Journal of the Taiwan Institute of Chemical Engineers, 62, 192–198. https://doi.org/10.1016/j.jtice.2016.02.004
4. Dehmani, Y., Alrashdi, A.A., Lgaz, H., Lamhasni, T., Abouarnadasse, S., Chung, I.M. 2020. Removal of phenol from aqueous solution by adsorption onto hematite (α-Fe2O3): Mechanism exploration from both experimental and theoretical studies. Arabian Journal of Chemistry, 13(5), 5474–5486. https://doi.org/10.1016/j.arabjc.2020.03.026
5. El Bakri, A., Ferraa, N., Rhilassi, A. El, Bennani-Ziatni, M. 2024. Resorcinol elimination through adsorption onto synthetic calcium phosphates: investigations into kinetics and thermodynamics. International Journal of Chemical and Biochemical Sciences (IJCBS), 25(13).
6. El Boujaady, H., El Rhilassi, A., Bennani-Ziatni, M., El Hamri, R., Taitai, A., Lacout, J.L. 2011. Removal of a textile dye by adsorption on synthetic calcium phosphates. Desalination, 275(1–3), 10–16. https://doi.org/10.1016/j.desal.2011.03.036
7. El Boujaady, H., Mourabet, M., Bennani-Ziatni, M., Taitai, A. 2014. Adsorption/desorption of Direct Yellow 28 on apatitic phosphate: Mechanism, kinetic and thermodynamic studies. Journal of the Association of Arab Universities for Basic and Applied Sciences, 16, 64–73. https://doi.org/10.1016/j.jaubas.2013.09.001
8. El Boujaady, H., Mourabet, M., El Rhilassi, A., Bennani-Ziatni, M., El Hamri, R., Taitai, A. 2017. Interaction of adsorption of reactive yellow 4 from aqueous solutions onto synthesized calcium phosphate. Journal of Saudi Chemical Society, 21, S94–S100. https://doi.org/10.1016/j.jscs.2013.10.009
9. El Rhilassi, A., Mourabet, M., El Boujaady, H., Bennani-Ziatni, M., Hamri, R. El, Taitai, A. 2012. Adsorption and release of amino acids mixture onto apatitic calcium phosphates analogous to bone mineral. Applied Surface Science, 259, 376–384. https://doi.org/10.1016/j.apsusc.2012.07.055
10. Fiamegos, Y., Stalikas, C., Pilidis, G. 2002.

4-Aminoantipyrine spectrophotometric method of phenol analysis Study of the reaction products via liquid chromatography with diode-array and mass spectrometric detection. Analytica Chimica Acta, 467.

11. Freundlich, H. 1926. Colloid and Capillary Chemistry, Methuen, London.
12. Giraldo, L., Moreno-Piraján, J.C. 2014. Study of adsorption of phenol on activated carbons obtained from eggshells. Journal of Analytical and Applied Pyrolysis, 106, 41–47. https://doi.org/10.1016/j.jaap.2013.12.007
13. Hameed, B.H., Ahmad, A.A., Aziz, N. 2007. Isotherms, kinetics and thermodynamics of acid dye adsorption on activated palm ash. Chemical Engineering Journal, 133(1–3), 195–203. https://doi.org/10.1016/j.cej.2007.01.032
14. Ho, Y.S., Mckay, G. 2000. The kinetics of sorption of divalent metal ions onto sphagnum moss peat. www.elsevier.com/locate/watres
15. Ho, Y.S., Mckay, G. 1999. Pseudo-second order model for sorption processes. Process Biochemistry, 34.
16. Hua, C., Zhang, R., Li, L., Zheng, X. 2012. Adsorption of phenol from aqueous solutions using activated carbon prepared from crofton weed. Desalination and Water Treatment, *37*(1–3), 230–237. https://doi.org/10.1080/19443994.2012.661277
17. Konggidinata, M.I., Chao, B., Lian, Q., Subramaniam, R., Zappi, M., Gang, D.D. 2017. Equilibrium, kinetic and thermodynamic studies for adsorption of BTEX onto Ordered Mesoporous Carbon (OMC). Journal of Hazardous Materials, 336, 249–259. https://doi.org/10.1016/j.jhazmat.2017.04.073
18. Lagergren, S. 1898. About the theory of so called adsorption of soluble substances, S. Vetenskapsakad, Hand. Band, 24(4), 1–39.
19. Langmuir, Irving, B. 1916. The evaporation, condensation and reflection of molecules and the mechanism of adsorption.
20. Li, H., Meng, F., Duan, W., Lin, Y., Zheng, Y. 2019. Biodegradation of phenol in saline or hypersaline environments by bacteria: A review. Ecotoxicology and Environmental Safety, Academic Press, 184. https://doi.org/10.1016/j.ecoenv.2019.109658
21. Lin, K., Pan, J., Chen, Y., Cheng, R., Xu, X. 2009. Study the adsorption of phenol from aqueous solution on hydroxyapatite nanopowders. Journal of Hazardous Materials, 161(1), 231–240. https://doi.org/10.1016/j.jhazmat.2008.03.076
22. Liu, Q.S., Zheng, T., Wang, P., Jiang, J.P., Li, N. 2010. Adsorption isotherm, kinetic and mechanism studies of some substituted phenols on activated carbon fibers. Chemical Engineering Journal, 157(2–3), 348–356. https://doi.org/10.1016/j.cej.2009.11.013
23. Liu, X., Tu, Y., Liu, S., Liu, K., Zhang, L., Li, G., Xu, Z. 2021. Adsorption of ammonia nitrogen and phenol onto the lignite surface: An experimental and molecular dynamics simulation study. Journal of Hazardous Materials, 416. https://doi.org/10.1016/j.jhazmat.2021.125966
24. Mahmoodi, N.M., Hayati, B., Arami, M., Lan, C. 2011. Adsorption of textile dyes on Pine Cone from colored wastewater: Kinetic, equilibrium and thermodynamic studies. Desalination, 268(1–3), 117–125. https://doi.org/10.1016/j.desal.2010.10.007
25. Michalowicz, J., Duda, W. 2007. Phenols – Sources and Toxicity. Polish J. of Environ. Stud., 16(3), 347–362.
26. Mishra, P., Singh, K., Dixit, U. 2021. Adsorption, kinetics and thermodynamics of phenol removal by ultrasound-assisted sulfuric acid-treated pea (Pisum sativum) shells. Sustainable Chemistry and Pharmacy, 22. https://doi.org/10.1016/j.scp.2021.100491
27. Mohammadi, S.Z., Darijani, Z., Karimi, M.A. 2020. Fast and efficient removal of phenol by magnetic activated carbon-cobalt nanoparticles. Journal of Alloys and Compounds, 832. https://doi.org/10.1016/j.jallcom.2020.154942
28. Mohammed, N.A.S., Abu-Zurayk, R.A., Hamadneh, I., Al-Dujaili, A.H. 2018. Phenol adsorption on biochar prepared from the pine fruit shells: Equilibrium, kinetic and thermodynamics studies. Journal of Environmental Management, 226, 377–385. https://doi.org/10.1016/j.jenvman.2018.08.033
29. Mourabet, M., El Rhilassi, A., El Boujaady, H., Bennani-Ziatni, M., El Hamri, R., Taitai, A. 2015. Removal of fluoride from aqueous solution by adsorption on hydroxyapatite (HAp) using response surface methodology. Journal of Saudi Chemical Society, 19(6), 603–615. https://doi.org/10.1016/j.jscs.2012.03.003
30. Nakhjiri, M.T., Bagheri Marandi, G., Kurdtabar, M. 2021a. Preparation of magnetic double network nanocomposite hydrogel for adsorption of phenol and p-nitrophenol from aqueous solution. Journal of Environmental Chemical Engineering, 9(2). https://doi.org/10.1016/j.jece.2021.105039
31. Nakhjiri, M.T., Bagheri Marandi, G., Kurdtabar, M. 2021b. Preparation of magnetic double network nanocomposite hydrogel for adsorption of phenol and p-nitrophenol from aqueous solution. Journal of Environmental Chemical Engineering, 9(2). https://doi.org/10.1016/j.jece.2021.105039
32. Norwitz, G., Bardsley, A.H., Keliher, P.N. 1981. Determination of Phenol in the Presence of Sulfite (Sulfur Dioxide) by the Aminoantipyrine Pectrophotometric Method. Analytica Chimica Acta, 128(1981), 251–256.
33. Rengaraj, S., Moon, S.-H., Sivabalan, R., Arabindoo, B., Murugesan, V. 2002. Removal of phenol from aqueous solution and resin manufacturing industry wastewater using an agricultural waste: rubber seed coat. Journal of Hazardous Materials, 89.

34. Sharafi, K., Pirsaheb, M., Gupta, V. K., Agarwal, S., Moradi, M., Vasseghian, Y., & Dragoi, E. N. (2019). Phenol adsorption on scoria stone as adsorbent - Application of response surface method and artificial neural networks. Journal of Molecular Liquids, 274, 699–714. https://doi.org/10.1016/j.molliq.2018.11.006
35. Tang, W., Huang, H., Gao, Y., Liu, X., Yang, X., Ni, H., Zhang, J. 2015. Preparation of a novel porous adsorption material from coal slag and its adsorption properties of phenol from aqueous solution. Materials and Design, 88, 1191–1200. https://doi.org/10.1016/j.matdes.2015.09.079
36. Tiewcharoen, S., Maihom, T., Sittiwong, J., Limtrakul, J. 2021. The influence of cation exchange and tetravalent metal substitutions in Lewis acidic BEA zeolites for phenol adsorption and Tautomerization: A computational study. Chemical Physics Letters, 780. https://doi.org/10.1016/j.cplett.2021.138886
37. Villar da Gama, B.M., Elisandra do Nascimento, G., Silva Sales, D.C., Rodríguez-Díaz, J.M., Bezerra de Menezes Barbosa, C.M., Menezes Bezerra Duarte, M.M. 2018. Mono and binary component adsorption of phenol and cadmium using adsorbent derived from peanut shells. Journal of Cleaner Production, 201, 219–228. https://doi.org/10.1016/j.jclepro.2018.07.291
38. Wang, T., Xu, Z.Y., Wu, L.G., Li, B.R., Chen, M.X., Xue, S.Y., Zhu, Y.C., Cai, J. 2017. Enhanced photocatalytic activity for degrading phenol in seawater by TiO2-based catalysts under weak light irradiation. RSC Advances, 7(51), 31921–31929. https://doi.org/10.1039/c7ra04732k
39. Wang, X., Hu, Y., Min, J., Li, S., Deng, X., Yuan, S., Zuo, X. 2018. Adsorption characteristics of phenolic compounds on graphene oxide and reduced graphene oxide: A batch experiment combined theory calculation. Applied Sciences (Switzerland), 8(10). https://doi.org/10.3390/app8101950
40. Wei, X., Gilevska, T., Wetzig, F., Dorer, C., Richnow, H.H., Vogt, C. 2016. Characterization of phenol and cresol biodegradation by compound-specific stable isotope analysis. Environmental Pollution, 210, 166–173. https://doi.org/10.1016/j.envpol.2015.11.005
41. Yon Oepen, B., K6rdel, W., Klein, W. 1991. Sorption of Nonpolar and Polar Compounds to Soils: Processes, Measurements and Experience with the Applicability of the Modified OECD-Guideline, 106, 22.
42. Zeboudj, S., Seiad, M. L., Namane, A., Hank, D., Hellal, A. (n.d.). Elimination du phenol : couplage de l'adsorption sur charbon actif et la biodegradation par pseudomonas aeruginosa. Rev. Microbiol. Ind. San et Environn., 8.
43. Zulfiqar, M., Sufian, S., Rabat, N.E., Mansor, N. 2020. Photocatalytic degradation and adsorption of phenol by solvent-controlled TiO2 nanosheets assisted with H2O2 and FeCl3: Kinetic, isotherm and thermodynamic analysis. Journal of Molecular Liquids, 308. https://doi.org/10.1016/j.molliq.2020.112941